

# UC Davis

## UC Davis Previously Published Works

### Title

$\beta$ 2AR Antagonists and  $\beta$ 2AR Gene Deletion Both Promote Skin Wound Repair Processes

### Permalink

<https://escholarship.org/uc/item/15c7m5xj>

### Journal

Journal of Investigative Dermatology, 132(8)

### ISSN

0022-202X

### Authors

Pullar, Christine E  
Le Provost, Gabrielle S  
O'Leary, Andrew P  
et al.

### Publication Date

2012-08-01

### DOI

10.1038/jid.2012.108

Peer reviewed

# $\beta$ 2AR Antagonists and $\beta$ 2AR Gene Deletion Both Promote Skin Wound Repair Processes

Christine E. Pullar<sup>1,2</sup>, Gabrielle S. Le Provost<sup>1</sup>, Andrew P. O'Leary<sup>1</sup>, Sian E. Evans<sup>1</sup>, Brian S. Baier<sup>2</sup> and R. Rivkah Isseroff<sup>2</sup>

Skin wound healing is a complex process requiring the coordinated, temporal orchestration of numerous cell types and biological processes to regenerate damaged tissue. Previous work has demonstrated that a functional  $\beta$ -adrenergic receptor autocrine/paracrine network exists in skin, but the role of  $\beta$ 2-adrenergic receptor ( $\beta$ 2AR) in wound healing is unknown. A range of *in vitro* (single-cell migration, immunoblotting, ELISA, enzyme immunoassay), *ex vivo* (rat aortic ring assay), and *in vivo* (chick chorioallantoic membrane assay, zebrafish, murine wild-type, and  $\beta$ 2AR knockout excisional skin wound models) models were used to demonstrate that blockade or loss of  $\beta$ 2AR gene deletion promoted wound repair, a finding that is, to our knowledge, previously unreported. Compared with vehicle-only controls,  $\beta$ 2AR antagonism increased angiogenesis, dermal fibroblast function, and re-epithelialization, but had no effect on wound inflammation *in vivo*. Skin wounds in  $\beta$ 2AR knockout mice contracted and re-epithelialized faster in the first few days of wound repair *in vivo*.  $\beta$ 2AR antagonism enhanced cell motility through distinct intracellular signalling mechanisms and increased vascular endothelial growth factor secretion from keratinocytes.  $\beta$ 2AR antagonism promoted wound repair processes in the early stages of wound repair, revealing a possible new avenue for therapeutic intervention.

*Journal of Investigative Dermatology* (2012) **132**, 2076–2084; doi:10.1038/jid.2012.108; published online 12 April 2012

## INTRODUCTION

Wound healing is a complex process requiring the coordinated, temporal orchestration of numerous cell types and processes to initiate repair (Shaw and Martin, 2009). The epidermis can synthesize and secrete a number of proteins (Boyce, 1994) including epinephrine (Schallreuter *et al.*, 1992; Pullar *et al.*, 2006b), a ligand for the  $\beta$ -adrenergic receptors ( $\beta$ ARs):  $\beta$ 1-adrenergic receptor ( $\beta$ 1AR),  $\beta$ 2AR, and  $\beta$ 3AR (Wallukat, 2002). They are G protein-coupled receptors highly expressed on all cell lineages in the skin (McSwigan *et al.*, 1981; Steinkraus *et al.*, 1992; Izeboud *et al.*, 1999; Iaccarino *et al.*, 2002; de Coupade *et al.*, 2004);

therefore, an autocrine and paracrine  $\beta$ AR network exists in the epidermis and dermis, respectively.

Previously, nonselective activation or blockade of the  $\beta$ ARs has revealed a regulatory role for  $\beta$ ARs in keratinocyte migration and re-epithelialization.  $\beta$ AR activation decreased the rate of human keratinocyte (HK) migration *in vitro* (Pullar *et al.*, 2003, 2006a; Pullar and Isseroff, 2005), whereas a  $\beta$ AR antagonist promoted HK migration, by blocking the autocrine epinephrine-mediated decrease in migration (Pullar *et al.*, 2006b). In excised human skin,  $\beta$ AR activation delayed wound re-epithelialization (Pullar *et al.*, 2006a), whereas  $\beta$ AR antagonism promoted skin re-epithelialization (Pullar *et al.*, 2006b) in an *ex vivo* model of chronic wound re-epithelialization (Kratz, 1998).

In murine skin wound models, stress-induced increases in epinephrine delayed wound repair (Sivamani *et al.*, 2009; Romana-Souza *et al.*, 2010a), whereas, conversely,  $\beta$ AR antagonism enhanced re-epithelialization in a murine skin burn model *in vivo* (Sivamani *et al.*, 2009) and accelerated skin barrier recovery (Denda *et al.*, 2003). In addition, a nonselective  $\beta$ AR antagonist improved wound healing in diabetic (Romana-Souza *et al.*, 2009a) and burn-injured (Romana-Souza *et al.*, 2008) rats and chronically stressed mice (Romana-Souza *et al.*, 2010b), while delaying repair in rat acute skin wounds (Souza *et al.*, 2006; Romana-Souza *et al.*, 2009c).

Here the effect of  $\beta$ 2AR antagonism and loss of the  $\beta$ 2AR on the main processes in wound repair were investigated. The *in vitro*, *ex vivo*, and *in vivo* models allowed a thorough

<sup>1</sup>Department of Cell Physiology and Pharmacology, University of Leicester, Leicester, UK; <sup>2</sup>Department of Dermatology, School of Medicine, University of California Davis, Davis, California, USA

Correspondence: Christine E. Pullar, University of Leicester, Department of Cell Physiology and Pharmacology, PO Box 138, University Road, Leicester LE1 9HN, UK. E-mail: cp161@le.ac.uk

Abbreviations:  $\beta$ AR,  $\beta$ -adrenergic receptor family;  $\beta$ 2AR,  $\beta$ 2-adrenergic receptor;  $\beta$ 2AR<sup>+/+</sup>, control wild-type mice;  $\beta$ 2AR<sup>-/-</sup>,  $\beta$ 2-AR knockout mice; BME, basement membrane extract; CAM, chick chorioallantoic membrane assay; EC, endothelial cell; ERK, extracellular signal-regulated kinase; HDF, human dermal fibroblast; HDMEC, human dermal microvascular endothelial cell; HK, human keratinocyte; MK, murine keratinocyte; MDF, murine dermal fibroblast; NHS, National Health Service; PMN, polymorphonuclear cell; SMA,  $\alpha$ -smooth muscle actin; SCM, single-cell migration; TH, tyrosine hydroxylase; VEGF, vascular endothelial growth factor

Received 10 October 2011; revised 27 January 2012; accepted 12 February 2012; published online 12 April 2012

mechanistic investigation of skin wound repair at both the cellular and the tissue level, using a combination of pharmacological and genetic approaches.

## RESULTS

### $\beta$ 2AR antagonism promotes angiogenesis

Angiogenesis is an essential process in acute wound healing (Tonnesen *et al.*, 2000), and endothelial cell (EC) migration is a critical process in angiogenesis (Eming *et al.*, 2007). To determine whether a  $\beta$ 2AR antagonist altered EC migration, single-cell migration (SCM) assays were performed with primary human dermal microvascular ECs (HDMECs) in the presence and absence of  $\beta$ 2AR antagonist; however, there was no effect on migration rate (Figure 1a).

To determine whether  $\beta$ 2AR antagonism could alter cell outgrowth from the cut edge of rat aorta (Smith and Staton, 2006), aortic pieces were embedded into the basement membrane extract and incubated in the presence or absence of a  $\beta$ 2AR antagonist for 5 days.  $\beta$ 2AR antagonism increased aortic outgrowth by 66% after 5 days (Figure 1b).

To investigate angiogenesis in a more complex, multi-cellular environment *in vivo*, the chick chorioallantoic membrane (CAM) assay, a model of embryonic angiogenesis (Smith and Staton, 2006), was selected.  $\beta$ 2AR antagonist treatment increased angiogenesis by 48% in the CAM assay, between days 5 and 9 post fertilization (Figure 1c).

Finally, to determine whether  $\beta$ 2AR antagonism could modulate wound angiogenesis *in vivo*, two full-thickness 6-mm wounds were created in the dorsal skin of wild-type ( $\beta$ 2AR<sup>+/+</sup>) and  $\beta$ 2AR knockout ( $\beta$ 2AR<sup>-/-</sup>) mice (Chruscinski *et al.*, 1999). The wounds were treated immediately after wounding and then daily, topically, with hydrogel alone or hydrogel containing 0.1%  $\beta$ 2AR antagonist, and photographed daily. To evaluate the amount of angiogenesis in the dermis, 7- $\mu$ m-thick sections from the wound center, excised after 5 days, were immunostained with an antibody to an EC marker (CD31), revealing the degree of angiogenesis in the mouse wounds (Yoon *et al.*, 2009).  $\beta$ 2AR antagonist treatment increased angiogenesis by 26% (Figure 1d). The amount of angiogenesis in  $\beta$ 2AR<sup>-/-</sup> wounds was equal to that observed in control  $\beta$ 2AR<sup>+/+</sup> wounds (Figure 1d), whereas  $\beta$ 2AR antagonist treatment of  $\beta$ 2AR<sup>-/-</sup> wounds had no effect (results not shown).

Vascular endothelial growth factor (VEGF) is a potent pro-angiogenic factor in acute wounds (Barrientos *et al.*, 2008), and  $\beta$ AR activation can increase VEGF expression in human choroid ECs (Steinle *et al.*, 2008). To determine whether  $\beta$ 2AR antagonism increased VEGF secretion from HDMECs, HKs, human dermal fibroblasts (HDFs), neutrophils, and macrophages, ELISAs were performed on control and  $\beta$ 2AR antagonist-treated supernatants. VEGF secretion was not detected in HDMECs or HDF supernatants. Although VEGF secretion was detected in the supernatants of neutrophils and macrophages,  $\beta$ 2AR antagonist treatment had no effect (results not shown). However,  $\beta$ AR antagonist treatment increased the amount of VEGF secreted from HKs after 24 hours by 23% (Figure 1e).

### $\beta$ 2AR antagonism promotes human dermal fibroblast migration *in vitro* and function *in vivo*

Within a few days of wounding, fibroblasts proliferate and migrate into the wound bed (Shaw and Martin, 2009). A nonselective  $\beta$ AR agonist increased HDF migration via the src-dependent transactivation of EGFR (Pullar and Isseroff, 2006). To determine the effect of  $\beta$ 2AR antagonism on HDF migration, SCM was performed in the presence and absence of a highly selective  $\beta$ 2AR antagonist.  $\beta$ 2AR antagonism increased the speed of HDF migration by 27% (Figure 2a). In addition, DFs were isolated from the skin of  $\beta$ 2AR<sup>+/+</sup> and  $\beta$ 2AR<sup>-/-</sup> mice. Although a  $\beta$ 2AR antagonist increased the migration speed of  $\beta$ 2AR<sup>+/+</sup> murine DFs (MDFs) by 49%, the speed of  $\beta$ 2AR<sup>-/-</sup> MDFs was increased by 46% compared with  $\beta$ 2AR<sup>+/+</sup> MDFs (Figure 2b). The  $\beta$ 2AR antagonist had no additional effect on  $\beta$ 2AR<sup>-/-</sup> MDF migration speed, as expected (Figure 2b). Extracellular signal-regulated kinase (ERK) has an important role in cell migration (Klemke *et al.*, 1997).  $\beta$ 2AR antagonism increased  $\beta$ 2AR<sup>+/+</sup> MDF ERK phosphorylation by 90% (Figure 2c).

To explore whether  $\beta$ 2AR antagonism could modulate wound DF function, two full-thickness 6-mm wounds were created in the dorsal skin of  $\beta$ 2AR<sup>+/+</sup> and  $\beta$ 2AR<sup>-/-</sup> mice and treated daily. Wound area was calculated daily until excision to determine the rate of wound contraction (Galiano *et al.*, 2004a), as described in the Materials and Methods section. Wound contraction was accelerated 4-fold in  $\beta$ 2AR antagonist-treated  $\beta$ 2AR<sup>+/+</sup> wounds and 5-fold in control  $\beta$ 2AR<sup>-/-</sup> wounds, 24 hours after wounding (Figure 3a). Wound contraction was still significantly enhanced by 2-fold in  $\beta$ 2AR antagonist-treated  $\beta$ 2AR<sup>+/+</sup> wounds and almost 3-fold in control  $\beta$ 2AR<sup>-/-</sup> wounds, 48 hours post wounding. After 3 days, contraction was increased by 19% in  $\beta$ 2AR antagonist-treated  $\beta$ 2AR<sup>+/+</sup> wounds and 40% in control  $\beta$ 2AR<sup>-/-</sup> wounds, but after 4 days, contraction of both  $\beta$ 2AR antagonist-treated  $\beta$ 2AR<sup>+/+</sup> wounds and control  $\beta$ 2AR<sup>-/-</sup> wounds occurred at the same rate as control  $\beta$ 2AR<sup>+/+</sup> wounds.  $\beta$ 2AR antagonist-treated  $\beta$ 2AR<sup>-/-</sup> wounds demonstrated the same rate of wound contraction as control  $\beta$ 2AR<sup>-/-</sup> wounds (Figure 3a).

Expression of  $\alpha$ -smooth muscle actin (SMA) is a reliable marker of myofibroblast differentiation, and the rate of wound contraction can directly correlate with SMA expression (Hinz *et al.*, 2001). Sections (7  $\mu$ m thick) from the wound center, excised after 5 days, were immunostained with an antibody to SMA. Populations of SMA-stained fibroblasts were observed below the wound epithelial margins, 5 days post wounding. The area of SMA staining was increased by 60% in  $\beta$ 2AR antagonist-treated wounds in  $\beta$ 2AR<sup>+/+</sup> mice and was similar in control  $\beta$ 2AR<sup>-/-</sup> and  $\beta$ 2AR<sup>+/+</sup> wounds (Figure 3b).

Myofibroblasts synthesize collagen III early in the wound repair process, which is later replaced by collagen I in more mature scars (Hinz, 2007). Sections (7  $\mu$ m thick) from the wound center, excised after 5 days, were immunostained with an antibody to collagen III.  $\beta$ 2AR antagonist treatment increased the area of collagen III-stained neo-dermis by 20% in  $\beta$ 2AR<sup>+/+</sup> wounds (Figure 3c), whereas control  $\beta$ 2AR<sup>-/-</sup> and  $\beta$ 2AR<sup>+/+</sup> wounds had similar areas of

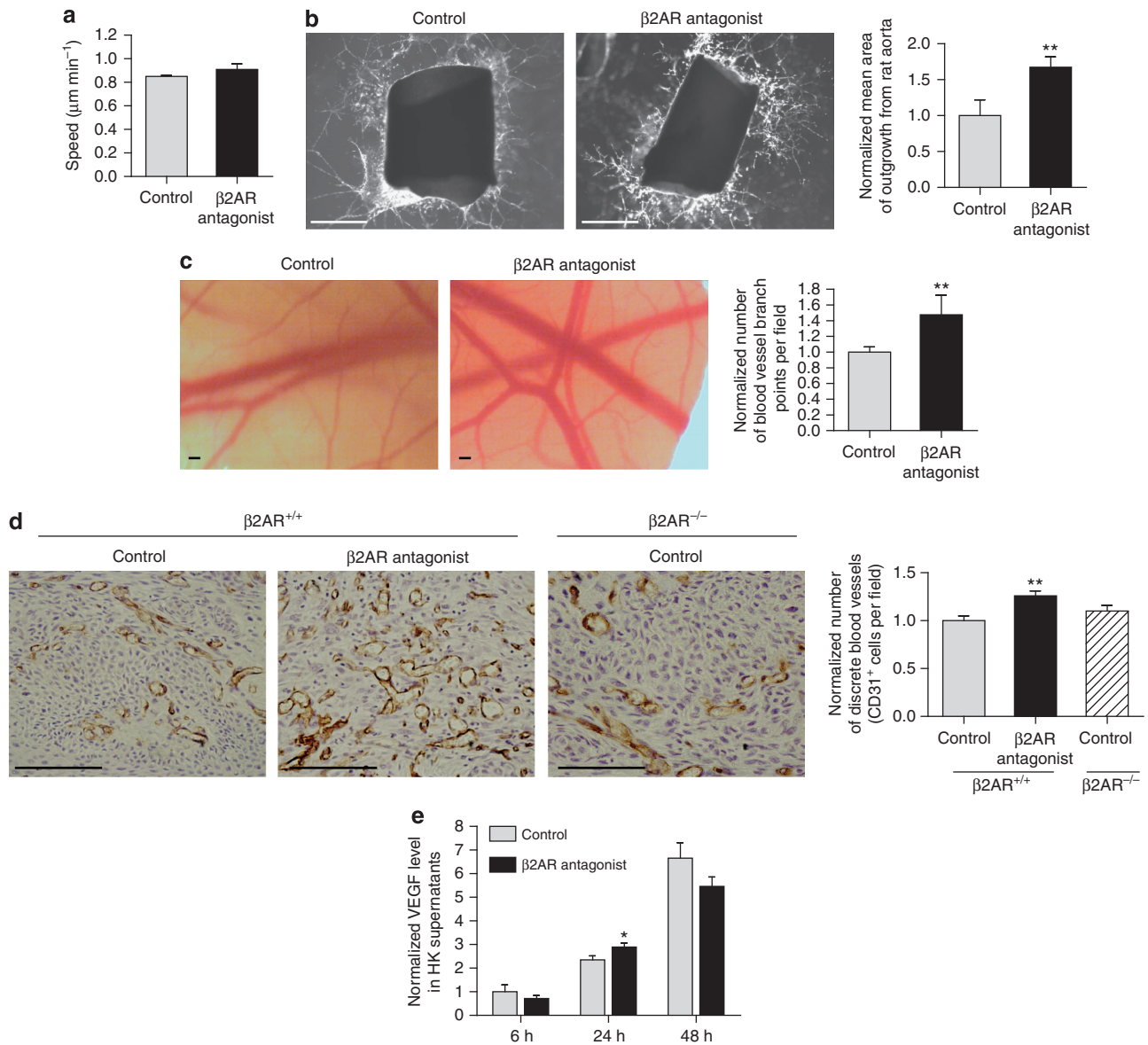


**Figure 1.  $\beta$ 2-Adrenergic receptor ( $\beta$ 2AR) antagonism promoted wound angiogenesis.** (a) Human dermal microvascular endothelial cells (HDMECs) were plated in the presence or absence of 10 nM  $\beta$ AR antagonist, and single-cell migration (SCM) was performed for 1 hour; see Materials and Methods (control,  $n = 200$ ; antagonist,  $n = 82$ ). (b) Rat aortic sections were prepared, incubated in the presence or absence of 10  $\mu$ M  $\beta$ AR antagonist, and imaged every 24 hours; see Materials and Methods. Representative images of aortas 5 days post-treatment are shown, bar = 1 mm. The area of outgrowth was measured using the Volocity software (control,  $n = 4$ ; antagonist,  $n = 4$ ). (c) Fertilized chicken eggs were prepared and chick chorioallantoic membranes (CAMs) were treated with vehicle alone or with vehicle containing 100  $\mu$ M  $\beta$ 2AR antagonist, from days 5 to 9, and imaged every 24 hours; see Materials and Methods. Representative day 9 images are shown, bar = 1 mm (control,  $n = 16$ ; antagonist,  $n = 3$ ). (d) Paraffin-embedded wound sections (7  $\mu$ m) from control and 0.1%  $\beta$ AR antagonist-treated wild-type ( $\beta$ 2AR<sup>+/+</sup>) mice and control  $\beta$ 2-AR knockout ( $\beta$ 2AR<sup>-/-</sup>) mice day 5 post wounding were immunostained with an anti-CD31 antibody; see Materials and Methods. Representative images are shown, bar = 100  $\mu$ m ( $n = 10$ –14). (e) Human keratinocytes (HKs) were plated for in the presence or absence of 10 nM  $\beta$ 2AR antagonist and prepared for vascular endothelial growth factor-A (VEGF-A) ELISA; see Materials and Methods. Data are representative of five independent experiments from two separate cell strains. Values plotted are the means  $\pm$  SEM. \* $P < 0.05$ ; \*\* $P < 0.01$ .

collagen III staining (Figure 3c). To examine this further, sections were stained with picosirius red to assess total collagen deposition in the neo-dermis (Junqueira *et al.*, 1979).  $\beta$ 2AR antagonist treatment increased the area of collagen-stained neo-dermis, within 1 mm<sup>2</sup> of the wound edge, by 29% in  $\beta$ 2AR<sup>+/+</sup> wounds (Figure 3d), whereas control  $\beta$ 2AR<sup>-/-</sup> and  $\beta$ 2AR<sup>+/+</sup> wounds had similar areas of collagen staining (Figure 3d).

**$\beta$ 2AR antagonism has no effect on wound inflammation *in vivo***  
Neutrophils and macrophages are recruited to the wound site to quell bacterial infections, where they secrete a cocktail of growth factors and cytokines to activate resident keratinocytes and fibroblasts (Martin, 1997).

To determine whether a  $\beta$ 2AR antagonist could alter the guidance of inflammatory cells to a wound, a zebrafish wound model was used. Indeed, zebrafish are known to have

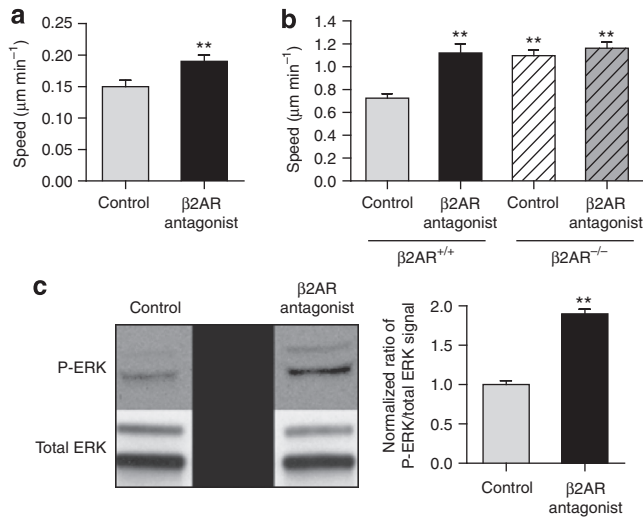


**Figure 2.  $\beta$ 2-Adrenergic receptor ( $\beta$ 2AR) antagonism, or the absence of  $\beta$ 2AR, increased dermal fibroblast (DF) migration.** (a) Human dermal fibroblasts (HDFs) were plated, single-cell migration (SCM) was performed for 1 hour, and the mean migration speed was calculated (HDF control,  $n = 107$ ;  $\beta$ 2AR antagonist,  $n = 112$ ). (b) Murine dermal fibroblasts (MDFs) were isolated from  $\beta$ 2AR knockout ( $\beta$ 2AR<sup>-/-</sup>) and wild-type ( $\beta$ 2AR<sup>+/+</sup>) neonates and SCM performed (MDF:  $\beta$ 2AR<sup>+/+</sup> control,  $n = 77$ , antagonist,  $n = 73$ ; MDF:  $\beta$ 2AR<sup>-/-</sup> control,  $n = 60$ ). (c) Confluent 35-mm<sup>2</sup> dishes of MDFs were stimulated for 10 minutes at 37 °C with media alone (control) or with media containing 10 nM ICI 118,551, samples were prepared, and western blotting performed for phosphorylated (P-) and total extracellular signal-regulated kinase (ERK); see Materials and Methods. The data shown are representative of three independent experiments. Three blots from separate experiments were scanned and densitometry performed; see Materials and Methods. Values plotted are the means  $\pm$  SEM. \*\* $P < 0.01$ .

two  $\beta$ 2AR genes (Steele *et al.*, 2011), but their role in tissue regeneration is unknown. Zebrafish larvae are transparent and zebrafish neutrophils are identifiable 48 hours post fertilization. Upon transection of the caudal fin, neutrophils are guided to the wound within minutes, but peak neutrophil recruitment occurs after approximately 6 hours (Renshaw *et al.*, 2006). When the wounded zebrafish larvae were immersed in pond water containing a  $\beta$ 2AR antagonist, there was no effect on neutrophil guidance to the caudal fin wound (Figure 4a).

To determine whether  $\beta$ 2AR antagonist treatment altered wound inflammation in the mouse excisional skin wound model, 7- $\mu\text{m}$ -thick sections from the wound center, excised after 3 days, were immunostained with either an antibody to a polymorphonuclear cell marker (Ly6G-6C) (Fleming *et al.*, 1993) or a macrophage marker (F4-80) (Austyn and Gordon, 1981). Topical  $\beta$ 2AR antagonist treatment or the absence of the receptor ( $\beta$ 2AR<sup>-/-</sup>) had no effect on the number of polymorphonuclear cells or macrophages recruited to the wound site either 3 or 5 days post wounding (Figure 4b and c; day 5 results not shown).

#### **$\beta$ 2AR antagonism promotes keratinocyte migration *in vitro* and re-epithelialization *in vivo***

Keratinocyte migration from the wound edges is a critical process to restore the barrier function of the epidermis, and

they are a valuable source for growth factors in the wound (Shaw and Martin, 2009).

A  $\beta$ 2AR antagonist increased keratinocyte migration significantly by 12% (Figure 5a). To confirm that murine keratinocytes (MKs) respond similarly to a  $\beta$ 2AR antagonist, MKs were isolated from newborn  $\beta$ 2AR<sup>+/+</sup> and  $\beta$ 2AR<sup>-/-</sup> mice and the effect of a  $\beta$ 2AR antagonist on motility was determined. A  $\beta$ 2AR antagonist enhanced MK SCM by 28% (Figure 5b).  $\beta$ 2AR<sup>-/-</sup> MKs migrated 16% faster than  $\beta$ 2AR<sup>+/+</sup> MKs, whereas a  $\beta$ 2AR antagonist had no additional effect on their migration, confirming the absence of the  $\beta$ 2AR (Figure 5b). A  $\beta$ 2AR antagonist-mediated 2.5-fold increase in ERK phosphorylation, known to have a pivotal role in pro-migratory signaling pathways (Klemke *et al.*, 1997), underpinned its effect on MK motility (Figure 5c).

Tyrosine hydroxylase, the enzyme controlling the rate-limiting step for catecholamine biosynthesis (Nagatsu *et al.*, 1964), was expressed in MKs (Figure 5d), and  $100 \pm 10$  and  $75 \pm 8 \text{ pg mg}^{-1}$  protein of epinephrine was measured by enzyme immunoassay in extracts from MKs. MKs similar to HKs (Pullar *et al.*, 2006b), therefore, can also synthesize epinephrine, generating an autocrine and paracrine adrenergic network in the murine epidermis and dermis, respectively.

Finally, to determine the effect of a  $\beta$ 2AR antagonist on wound re-epithelialization, 7- $\mu\text{m}$ -thick sections from the wound center, excised after 3 and 5 days, were stained with hematoxylin and eosin, and the linear distance covered by new epithelium was determined.  $\beta$ 2AR antagonist treatment increased  $\beta$ 2AR<sup>+/+</sup> wound re-epithelialization by 60 and 56% within 3 and 5 days post wounding, respectively (Figure 5e). In addition, re-epithelialization of  $\beta$ 2AR<sup>-/-</sup> wounds was increased by 64% 5 days post wounding (Figure 5e).

#### **DISCUSSION**

$\beta$ 2AR antagonism enhanced angiogenesis *ex vivo* and *in vivo* and increased VEGF secretion from HKs.  $\beta$ 2AR antagonism increased the migration rate of HDFs *in vitro*, while increasing SMA expression, collagen III expression, and contractile ability in murine wounds *in vivo*. In addition,  $\beta$ 2AR<sup>-/-</sup> wounds contracted faster in the first few days post wounding. In contrast,  $\beta$ 2AR antagonism had no effect on wound inflammation *in vivo*. Finally,  $\beta$ 2AR antagonism or loss of  $\beta$ 2AR increased keratinocyte migration *in vitro* and promoted re-epithelialization *in vivo* within 5 days of wounding. In summary,  $\beta$ 2AR antagonism promoted wound repair, as summarized in the Supplementary Appendix S1 online.

In previous studies, a nonselective  $\beta$ AR antagonist, propranolol, improved healing in hospitalized burn patients, because of its ability to decrease energy expenditure and muscle protein catabolism (Mohammadi *et al.*, 2009) and improved wound repair in rabbit skin wounds (Zhang *et al.*, 2009), diabetic rats (Romana-Souza *et al.*, 2009b), and burn-injured rats (Romana-Souza *et al.*, 2008). The studies presented here use a highly selective  $\beta$ 2AR antagonist, ICI 118,551 (Bilski *et al.*, 1983), demonstrating for the first time that selective blockade of the  $\beta$ 2AR promotes wound

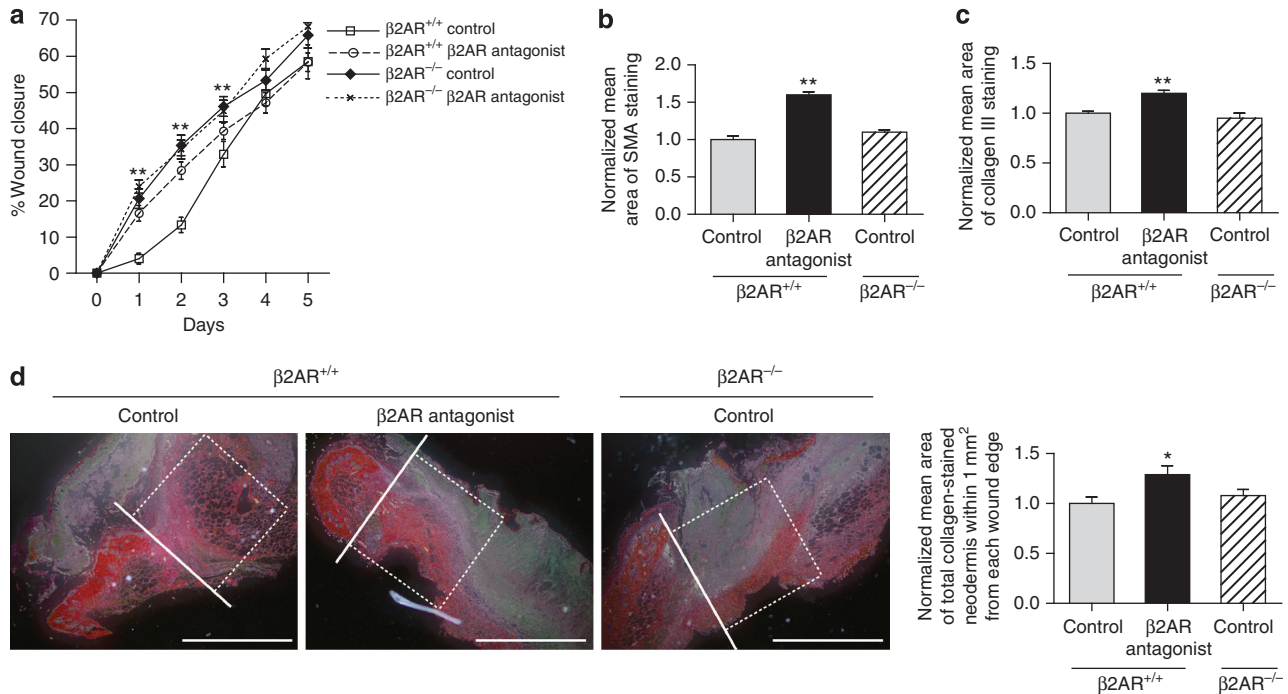


**Figure 3.  $\beta$ 2-Adrenergic receptor ( $\beta$ 2AR) antagonism, or the absence of  $\beta$ 2AR, increased dermal fibroblast function *in vivo*.** (a) Two full-thickness 6-mm excisional wounds, created in the dorsal skin of  $\beta$ 2-AR wild-type ( $\beta$ 2AR<sup>+/+</sup>) and  $\beta$ 2-AR knockout ( $\beta$ 2AR<sup>-/-</sup>) mice, were treated and photographed daily, and the area of each wound was calculated; see Materials and Methods. Sections (7  $\mu$ m), day 5 post wounding, were stained with (b) an anti-smooth muscle actin (SMA) antibody or (c) an anti-collagen III antibody. The mean area of positive staining was calculated; see Materials and Methods. (d) Representative images of picrosirius red staining are shown. The mean area of collagen-stained neo-dermis within (white square) 1 mm<sup>2</sup> of the (white line) wound edge was calculated; see Materials and Methods. Bar = 1 mm (*n* = 10–14). Values plotted are means  $\pm$  SEM. \**P* < 0.05; \*\**P* < 0.01.

processes, including angiogenesis, DF function, and re-epithelialization, thus accelerating healing.

The mechanism underpinning the  $\beta$ 2AR antagonist-mediated increase in angiogenesis could be partly attributed to the  $\beta$ 2AR antagonist-mediated increase in VEGF secretion from HKs, known to be an important source of VEGF (Rossiter *et al.*, 2004) and other growth factors in wounds (Werner and Grose, 2003; Barrientos *et al.*, 2008). Indeed, the addition of autologous cultured keratinocytes can aid healing of chronic venous leg ulcers (Liu *et al.*, 2004) and the addition of VEGF promotes healing in chronic diabetic wounds (Galiano *et al.*, 2004b; Brem *et al.*, 2009); therefore, the  $\beta$ 2AR antagonist-mediated increase in HK VEGF secretion could be highly beneficial for wound repair. In the complex wound environment,  $\beta$ 2AR antagonist treatment could also increase the secretion of other pro-angiogenic factors such as fibroblast growth factor 2 or basic fibroblast growth factor or platelet-derived growth factor (Battagay *et al.*, 1994), from wound cells, which could contribute to the enhanced angiogenesis observed *in vivo*. In contrast, post-ischemic angiogenesis was impaired in  $\beta$ 2AR<sup>-/-</sup> mice (Ciccarelli *et al.*, 2011).

The increase in wound contraction observed in  $\beta$ 2AR<sup>-/-</sup> wounds (Figure 3a) occurred in the absence of an increase in SMA-expressing cells in the wound bed (Figure 3b), in contrast to the observed increase in both wound contraction and SMA expression in the  $\beta$ 2AR antagonist-treated  $\beta$ 2AR<sup>+/+</sup> wounds. Although the rate of wound contraction is thought to correlate directly with SMA expression (Hinze *et al.*,

2001), there are several reports describing that wound contraction can occur in the absence of SMA-expressing myofibroblasts. Wounds in vanadate-treated rats (Ehrlich *et al.*, 1999) and rat wounds treated with a Smad blocker, SB-505124 (Au and Ehrlich, 2010), contracted normally, but SMA-expressing cells were not detected in the granulation tissue. Finally, a personal communication from JJ Tomasek reports that SMA knockout mice heal normally (Hinze, 2007). It appears that wound contraction is not correlated with SMA expression in  $\beta$ 2AR<sup>-/-</sup> mouse wounds and only  $\beta$ 2AR antagonist treatment can increase SMA expression (Figure 3b).

In addition, blockade of autocrine, endogenously synthesized epinephrine (Figure 5d), inhibitory to keratinocyte migration (Pullar *et al.*, 2003, 2006a), likely contributed to the ability of the  $\beta$ 2AR antagonist to promote MK migration *in vitro* and re-epithelialization *in vivo*.

Although  $\beta$ 2AR antagonist treatment did not alter acute wound inflammation or the secretion of VEGF from inflammatory cells,  $\beta$ 2AR blockade has been demonstrated to attenuate the hyper-inflammatory response to traumatic injury in mice (Rough *et al.*, 2009). It is possible, therefore, that  $\beta$ 2AR antagonist treatment could reduce persistent or hyper-inflammation, which will be tested in a chronic wound model.

In conclusion, here we report that  $\beta$ 2AR antagonism promotes wound angiogenesis, DF function, and re-epithelialization, enhancing wound repair, thus revealing a possible new avenue of therapeutic intervention. To our knowledge, this is previously unreported.

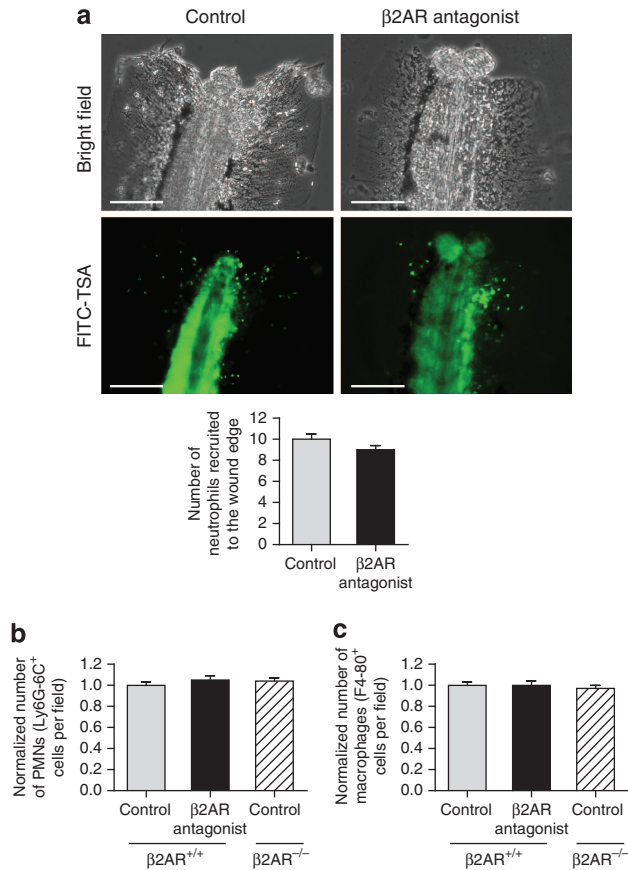


**Figure 4. β2-Adrenergic receptor (β2AR) antagonism has no effect on wound inflammation.** Zebrafish larvae were wounded, untreated, or treated with 500 μM β2AR antagonist and imaged using fluorescein-tyramine signal amplification; see Materials and Methods. (a) The number of neutrophils recruited to each wounded tail was recorded. Bar = 100 μm ( $n = 15-30$ ). Paraffin-embedded murine wound sections (7 μm), day 3 post wounding, were immunostained with an antibody that recognizes (b) neutrophils (Ly6G-6C) or (c) macrophages (F4-80). The positive cells per field were counted and the data analyzed from 10 images of each wound section; see Materials and Methods ( $n = 10-14$ ). Values plotted are means ± SEM. FITC, fluorescein isothiocyanate; PMNs, polymorphonuclear cells; TSA, tyramide signal amplification.

## MATERIALS AND METHODS

### Animals

The β2AR-deficient FVB/N (β2AR<sup>-/-</sup>) mice were a kind gift from Dr Brian Kobilka, Stanford University (Stanford, CA) (Chruscinski *et al.*, 1999). The congenic controls, FVB/N (β2AR<sup>+/+</sup>) mice, were purchased from The Jackson Laboratory (Bar Harbor, ME). The genotypes of the β2AR<sup>+/+</sup> and β2AR<sup>-/-</sup> mice were confirmed by PCR, using published primers (Chruscinski *et al.*, 1999). All animals used in the study were females between 8 and 12 weeks of age. The University of California, Davis Institutional Animal Care and Use Committee (IACUC) approved all animal protocols.

Adult zebrafish were maintained, as described (Westerfield, 1994), in compliance with the Animals (Scientific Procedures; www.legislation.gov.uk/ukpga/1986/14/contents) Act, 1986. Embryos were harvested and raised in egg water (Westerfield, 1994), at 28.5 °C, until the required developmental stage. Staging was performed in accordance with (Kimmel *et al.*, 1995).

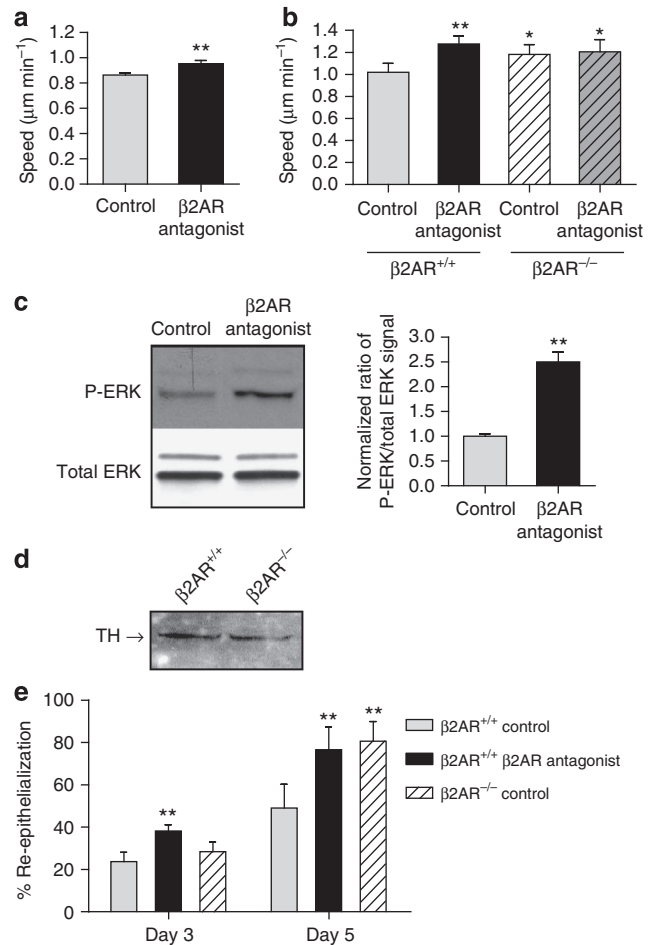


**Figure 5. β2-Adrenergic receptor (β2AR) antagonism, or the absence of β2AR, increased keratinocyte migration and re-epithelialization.** (a) Human keratinocytes (HKs) and (b) murine keratinocytes (MKs), isolated from β2AR knockout (β2AR<sup>-/-</sup>) and wild-type (β2AR<sup>+/+</sup>) neonates, were plated and single-cell migration (SCM) performed; see Materials and Methods (HK: control,  $n = 224$ , antagonist,  $n = 179$ ; MK: β2AR<sup>+/+</sup> control,  $n = 128$ , β2AR antagonist,  $n = 102$ ; β2AR<sup>-/-</sup> control = 105). MKs were treated with media alone (control) or with media containing 10 nM β2AR antagonist, and western blotting for extracellular signal-regulated kinase (ERK) was performed; see Materials and Methods. (c) Blots were scanned and densitometry performed using NIH Image J. (d) MK lysates were prepared and western blotting for tyrosine hydroxylase (TH) was performed. The data shown are representative of three independent experiments. Control and β2AR antagonist-treated β2AR<sup>+/+</sup> wounds and control β2AR<sup>-/-</sup> wounds were excised, fixed, and stained. The percentage of wound re-epithelialization, at days 3 and 5 post wounding, was calculated using Image J; see Materials and Methods ( $n = 10$ ) (e). Values plotted are means ± SEM. \* $P < 0.05$ ; \*\* $P < 0.01$ . P-ERK, phosphorylated-ERK.

### Culture of primary cells

Primary MKs were isolated from newborn mouse pups, as described previously (Isseroff *et al.*, 1983), and cultured in MK growth media (Epilife and keratinocyte growth supplement), 10 ng ml<sup>-1</sup> murine EGF, 0.1 nM cholera toxin (Invitrogen, Paisley, UK), and 0.5% antibiotic solution (25 U ml<sup>-1</sup> penicillin and 25 μg ml<sup>-1</sup> streptomycin (Sigma Aldrich, Poole, UK), murine keratinocyte complete growth medium). To isolate MDFs, the remaining dermal pieces were minced with sterile scissors and transferred to 100-mm plastic cell culture dishes from Falcon Labware (BD Biosciences, Oxford, UK).

Dermal pieces were allowed to attach for 5 minutes, before the addition of 4 ml of fibroblast growth medium, which consists of DMEM (basal medium), 0.5% antibiotic solution (25 U ml<sup>-1</sup> penicillin and 25  $\mu$ g ml<sup>-1</sup> streptomycin; Sigma Aldrich), and 10% fetal calf serum (Invitrogen). The plates were incubated at 37 °C in a humidified atmosphere of 5% CO<sub>2</sub> for 48 hours before adding an additional 6 ml of fibroblast growth medium per dish.

Primary human neonatal DFs were purchased from Invitrogen and cultured as described previously (Pullar and Isseroff, 2006).

Primary HDMECs were purchased from Invitrogen. Cells were grown in EC growth media supplemented with microvascular growth supplement (PromoCell, Heidelberg, Germany) and antibiotics (25 U ml<sup>-1</sup> penicillin, 25  $\mu$ g ml<sup>-1</sup> streptomycin; Invitrogen) at 37 °C with 5% CO<sub>2</sub>/95% air in a humidified atmosphere. Cells were grown on attachment factor containing 0.1% gelatin (Invitrogen), and experiments were conducted using cell passages between 3 and 7.

Primary neonatal HKs were purchased from Invitrogen and cultured as described previously (Pullar and Isseroff, 2005). At least three keratinocytes strains, between passages 3 and 6, were used in all experiments.

#### SCM assay

Plastic cell culture dishes (35 mm) were coated with collagen I (60  $\mu$ g ml<sup>-1</sup>) (Invitrogen) in phosphate-buffered saline for 1 hour at 37 °C. MDFs, isolated from both  $\beta$ 2AR<sup>-/-</sup> and  $\beta$ 2AR<sup>+/+</sup> mice, and HDFs were plated at a density of 25 cells per mm<sup>2</sup> in fibroblast growth medium, whereas MKs, HKs, and HDMECs were plated at a density of 50 cells per mm<sup>2</sup>, in their appropriate complete media (see culture methods), for 2 hours at 37 °C. Cells were incubated with complete media alone (control) or with media containing 10 nM  $\beta$ 2AR antagonist (ICI 118,551; Tocris Biosciences, Bristol, UK) at time 0. The 35-mm dishes were placed in a heating chamber, designed to maintain the medium at 37 °C, and images were taken every 10 minutes for 1 hour with the Improvise software (Perkin Elmer, Cambridge, UK), as described previously (Pullar *et al.*, 2006b).

#### Cell treatments for immunoblotting

MKs or MDFs plated at a density of  $1 \times 10^6$ , isolated from both  $\beta$ 2AR<sup>-/-</sup> and  $\beta$ 2AR<sup>+/+</sup> mice, were incubated with either murine keratinocyte complete growth medium (MK) or fibroblast growth medium (MDF) alone (control and lysates for catecholamine synthesis enzyme detection), or with media containing 10 nM  $\beta$ 2AR antagonist (ICI, 118551), for 10 minutes. Lysates were prepared and electrophoresed, as previously described for phosphorylated and total ERK (Pullar *et al.*, 2003) and tyrosine hydroxylase (Pullar *et al.*, 2006b).

#### Enzyme immunoassay for the quantitative determination of epinephrine in small sample volumes

MKs ( $1 \times 10^7$ ), isolated from both  $\beta$ 2AR<sup>-/-</sup> and  $\beta$ 2AR<sup>+/+</sup> mice, were extracted in 100  $\mu$ l 0.1 N HCl and sonicated on ice for 10 minutes. Extracts were tested in triplicate in an epinephrine enzyme immunoassay (Invitrogen) according to the manufacturer's instructions.

#### ELISA

Cells were plated on collagen I (30  $\mu$ g ml<sup>-1</sup>)-coated 6-well plates and incubated for 24 hours in the appropriate complete media to reach 70/80% confluence. Cells were washed with Hank's balanced salt solution and serum starved for 24 hours in the appropriate basal

media. Cells were then incubated with either basal media alone or media containing 10  $\mu$ M  $\beta$ 2AR antagonist for 6, 24, or 48 hours. After each time point, media were collected and stored at -80 °C for analysis with a Duoset VEGF-A ELISA kit (R&D Systems, Abingdon, UK).

#### Rat aortic ring assay

Animals were killed using an approved schedule 1 method. The abdominal and aortic arcs were extracted from adult Wistar rats and placed into sterile phosphate-buffered saline. The fibro-adipose tissue was then removed, and the aortas were washed in warm, sterile phosphate-buffered saline three times. Aortas were cut into uniform, 1-mm sections, placed into 80  $\mu$ l of basement membrane extract (R&D Systems), and incubated at 37 °C for 30 minutes. Aortas were incubated in EC basal media supplemented with 2% microvascular growth supplement for 3 days, and then with media alone or media containing 10  $\mu$ M  $\beta$ 2AR antagonist (ICI 118,551) for a further 5 days. Aortic endothelial outgrowth was imaged every 24 hours, using a Nikon eclipse microscope and the Improvise Openlab software. The area of outgrowth was analyzed using the Improvise Volocity software.

#### Zebrafish caudal fin wound model

Zebrafish larvae, 72 hours post-fertilization, were immersed in pond water containing 2% tricaine, and complete transection of the tail was performed with a sterile scalpel blade. After wounding, the larvae were incubated in the presence or absence of 500  $\mu$ M  $\beta$ 2AR antagonist (ICI 118,551) for 6 hours, and washed and stained using a fluorescein-tyramide signal amplification method (Perkin Elmer) before fixation in 4% paraformaldehyde. Tails were mounted and photographed on a Nikon TE-2000E inverted microscope at  $\times 20$  magnification using a fluor objective. The number of neutrophils recruited to each wounded tail was recorded.

#### CAM assay

Fertilized eggs were obtained, 1 day post fertilization, from local hatcheries and incubated at 37 °C in a humidified environment for 48 hours. On day 3, approximately 5 ml of albumin was removed from the obtuse poles of the eggs using a 21 G cannula. A square window (2  $\times$  2 cm<sup>2</sup>) was opened into the shell and shell membrane using a Dremel tool (Dremel, Uxbridge, UK). The window was then sealed with Parafilm and incubated horizontally for 48 hours at 37 °C. On day 5, water or 100  $\mu$ M  $\beta$ 2AR antagonist (ICI 118,551) in water was evaporated onto the center of a sterile 13-mm coverslip and then placed face down onto the CAM. CAMs were photographed through the coverslip center, every 24 hours, until day 9 using a stereomicroscope (Prior Scientific, Cambridge, UK). Angiogenesis was analyzed by counting the total number of branch points per field of view through the center of the coverslip.

#### Murine wound model

$\beta$ 2AR<sup>-/-</sup> and  $\beta$ 2AR<sup>+/+</sup> mice were anesthetized by intraperitoneal injection of ketamine (100 mg kg<sup>-1</sup>)/xylazine (10 mg kg<sup>-1</sup>) (Pfizer, Sandwich, UK). Back skin was shaved and two circular, full-thickness 6-mm excisional wounds were created 2 cm apart, in the center of the back, using a sterile 6-mm biopsy punch (SMS, Camberley, UK) to mark the skin for surgical excision. Wounds were treated topically with 100  $\mu$ l of hydrogel alone (Duoderm, ConvaTec, Uxbridge, UK) or containing 0.1% (1 mM) selective  $\beta$ 2AR antagonist (ICI 118,551)



(a concentration previously demonstrated to accelerate mouse epidermal barrier recovery; Denda *et al.*, 2003) immediately after wounding and daily thereafter until harvesting ( $n=5-7$  mice per group, two wounds per mouse). Each mouse was housed separately after wounding until wound harvest. Wounds were left uncovered and digitally photographed, daily, to determine wound contraction over time. Wounds were harvested 3 and 5 days post wounding by carefully applying an 8-mm punch (SMS) around the original wound and lightly pressing to form an outline on the skin. Scissors were used to excise the wound without damaging the delicate wound bed.

For histological analysis, the wounds were fixed in an IHC zinc fixative (BD Biosciences). The zinc-fixed biopsies were bisected, to ensure that sections were taken from the center of the wound, dehydrated through an ethanol-xylene series, and embedded in paraffin. Cross-sections, 7 μm thick, were stained with the hematoxylin-eosin technique or with picosirius red, to visualize collagen in the neo-dermis (Junqueira *et al.*, 1979), as described by Dapson *et al.* (2011). Sections were immunostained with an antibody against SMA (Dako, Ely, UK), collagen III (Rockland, Lorne Laboratories, Reading, UK), Ly6G-6C (a neutrophil marker; BD Pharmingen, Oxford, UK), F4-80 (a macrophage marker; Serotec, Kidlington, UK), or CD31 (an EC marker; BD Pharmingen), followed by DAB detection (BD Pharmingen) according to the manufacturer's protocols.

Specimens that were damaged in the histological process or otherwise non-interpretible were excluded from the study. Re-epithelialization was determined by examining all hematoxylin- and eosin-stained sections by light microscopy, using a Q-imaging Retiga-EX camera attached to a Nikon T-100 inverted microscope, controlled by the Improvise software. Image J was used to measure the linear distance covered by new epithelium and the linear distance between the original wound edges, to determine the percentage of re-epithelialization. Wound closure was quantified by measuring the wound area of each wound from the digital pictures taken every day with Image J. Each picture was calibrated individually. Images of picosirius red-stained sections were captured on an Olympus BX51 upright microscope equipped for dark field. The area of the collagen-stained neo-dermis was analyzed by measuring the red-stained area within 1 mm<sup>2</sup> of each wound edge on the dark-field pictures with the Image J software. Images of the SMA-stained wounds were captured on a Nikon SMZ-U upright microscope with the Nikon ACT-1 software. Images of the collagen III-stained wounds were captured on a Nikon Eclipse inverted microscope with the NIS-Elements software. NIH Image J was used to determine the area of SMA and collagen III staining in each wound to calculate the mean area of SMA and collagen III staining in each group. Images of the CD31- ( $\times 40$  magnification), Ly-6G-6C-, and F4-80-stained ( $\times 60$  magnification) wounds were also captured on the Nikon Eclipse microscope. The number of stained cells/vessels in each image was counted in a double-blind manner, and the average cell/vessel number was calculated for each group. For all image analysis, 10 fields were selected from the dermis below the wound margins and across the wound bed using a template to ensure that images were captured from similar areas in each wound.

### Statistical analysis

Unless mentioned in a specific method, categorical variables were compared with a two-tailed Fisher's exact test or a one-way analysis of variance, followed by the Dunnett's test, whereas each continuous

variable test group was compared with the control using the two-tailed Student's *t*-test for unpaired data with unequal variance.  $P < 0.05$  (\*) was significant and  $P < 0.01$  (\*\*) highly significant.

### CONFLICT OF INTEREST

CEP/RRI are coinventors on a patent held at University of California, Davis, entitled "β2AR modulation of wound healing". The authors declare that there are no other competing interests.

### ACKNOWLEDGMENTS

We thank Maggie Chiu for her assistance with the processing of the tissue for immunohistochemistry. We acknowledge the help of Dr Jonathan McDermid, University of Leicester, for help with staging the zebrafish embryos. We also thank Professor Andrew Wardlaw for providing the isolated human neutrophils. The work was performed in their laboratories, which are partly funded by ERDF no. 05567. *Financial disclosure:* No funding bodies had any role in the study design, data collection and analysis, decision to publish, or preparation of the manuscript. This work was supported by an NIH, NIAMS (<http://www.niams.nih.gov>) career award grant AR48827 (CEP); a Wellcome Trust (<http://www.wellcome.ac.uk>) grant 85586 (CEP), an MRC (<http://www.mrc.ac.uk>) grant G0901844 (CEP), and a BSF (<http://www.britishskin-foundation.org.uk>) grant 929 s (CEP); an NIH grant AR44518 (RRI); and a Shriners' Hospitals grant 8550 (RRI).

### Author contributions

CEP and RRI initiated the concept for the murine wound study. RRI contributed to the initial analysis of the murine wound study and the proofreading of the final article. CEP initiated the concept for all mechanistic studies, designed, acquired, analyzed, and interpreted the majority of the data, and drafted and revised the article. GSLP, APO, SE, and BB substantially contributed to the design of some experiments, the acquisition, analysis, and interpretation of the majority of the associated data, and either the drafting or the proofreading of the article.

### SUPPLEMENTARY MATERIAL

Supplementary material is linked to the online version of the paper at <http://www.nature.com/jid>

### REFERENCES

- Au K, Ehrlich HP (2010) When the Smad signaling pathway is impaired, fibroblasts advance open wound contraction. *Exp Mol Pathol* 89:236-40
- Austyn JM, Gordon S (1981) F4/80, a monoclonal antibody directed specifically against the mouse macrophage. *Eur J Immunol* 11:805-15
- Barrientos S, Stojadinovic O, Golinko MS *et al.* (2008) Growth factors and cytokines in wound healing. *Wound Repair Regen* 16:585-601
- Battegay EJ, Rupp J, Iruela-Arispe L *et al.* (1994) PDGF-BB modulates endothelial proliferation and angiogenesis *in vitro* via PDGF beta-receptors. *J Cell Biol* 125:917-28
- Bilski AJ, Halliday SE, Fitzgerald JD *et al.* (1983) The pharmacology of a beta 2-selective adrenoceptor antagonist (ICI 118,551). *J Cardiovasc Pharmacol* 5:430-7
- Boyce ST (1994) Epidermis as a secretory tissue. *J Invest Dermatol* 102:8-10
- Brem H, Kodra A, Golinko MS *et al.* (2009) Mechanism of sustained release of vascular endothelial growth factor in accelerating experimental diabetic healing. *J Invest Dermatol* 129:2275-87
- Chruscinski AJ, Rohrer DK, Schauble E *et al.* (1999) Targeted disruption of the beta2 adrenergic receptor gene. *J Biol Chem* 274:16694-700
- Ciccarelli M, Sorriento D, Cipolletta E *et al.* (2011) Impaired neoangiogenesis in beta-adrenoceptor gene-deficient mice: restoration by intravascular human beta-adrenoceptor gene transfer and role of NFκB and CREB transcription factors. *Br J Pharmacol* 162:712-21
- Dapson RW, Fagan C, Kiernan JA *et al.* (2011) Certification procedures for sirius red F3B (CI 35780, Direct red 80). *Biotech Histochem* 86:133-9
- de Coupade C, Gear RW, Dazin PF *et al.* (2004) Beta 2-adrenergic receptor regulation of human neutrophil function is sexually dimorphic. *Br J Pharmacol* 143:1033-41

- Denda M, Fuziwara S, Inoue K (2003) Beta2-adrenergic receptor antagonist accelerates skin barrier recovery and reduces epidermal hyperplasia induced by barrier disruption. *J Invest Dermatol* 121:142–8
- Ehrlich HP, Keefer KA, Myers RL et al. (1999) Vanadate and the absence of myofibroblasts in wound contraction. *Arch Surg* 134:494–501
- Eming SA, Brachvogel B, Odorisio T et al. (2007) Regulation of angiogenesis: wound healing as a model. *Progr Histochem Cytochem* 42:115–70
- Fleming TJ, Fleming ML, Malek TR (1993) Selective expression of Ly-6G on myeloid lineage cells in mouse bone marrow. RB6-8C5 mAb to granulocyte-differentiation antigen (Gr-1) detects members of the Ly-6 family. *J Immunol* 151:2399–408
- Galiano RD, Michaels JT, Dobryansky M et al. (2004a) Quantitative and reproducible murine model of excisional wound healing. *Wound Repair Regen* 12:485–92
- Galiano RD, Tepper OM, Pelo CR et al. (2004b) Topical vascular endothelial growth factor accelerates diabetic wound healing through increased angiogenesis and by mobilizing and recruiting bone marrow-derived cells. *Am J Pathol* 164:1935–47
- Hinz B (2007) Formation and function of the myofibroblast during tissue repair. *J Invest Dermatol* 127:526–37
- Hinz B, Celetta G, Tomasek JJ et al. (2001) Alpha-smooth muscle actin expression upregulates fibroblast contractile activity. *Mol Biol Cell* 12:2730–41
- Iaccarino G, Cipolletta E, Fiorillo A et al. (2002) Beta(2)-adrenergic receptor gene delivery to the endothelium corrects impaired adrenergic vasorelaxation in hypertension. *Circulation* 106:349–55
- Isseroff RR, Fusenig NE, Rifkin DB (1983) Plasminogen activator in differentiating mouse keratinocytes. *J Invest Dermatol* 80:217–22
- Izaboud CA, Mocking JA, Monshouer M et al. (1999) Participation of beta-adrenergic receptors on macrophages in modulation of LPS-induced cytokine release. *J Recept Signal Transduct Res* 19:191–202
- Junqueira LC, Bignolas G, Brentani RR (1979) Picrosirius staining plus polarization microscopy, a specific method for collagen detection in tissue sections. *Histochem J* 11:447–55
- Kimmel CB, Ballard WW, Kimmel SR et al. (1995) Stages of embryonic development of the zebrafish. *Dev Dyn* 203:253–310
- Klemke RL, Cai S, Giannini AL et al. (1997) Regulation of cell motility by mitogen-activated protein kinase. *J Cell Biol* 137:481–92
- Kratz G (1998) Modeling of wound healing processes in human skin using tissue culture. *Microsc Res Technol* 42:345–50
- Liu JY, Hafner J, Dragieva G et al. (2004) Autologous cultured keratinocytes on porcine gelatin microbeads effectively heal chronic venous leg ulcers. *Wound Rep Reg* 12:148–56
- Martin P (1997) Wound healing—aiming for perfect skin regeneration. *Science* 276:75–81
- McSwigan JD, Hanson DR, Lubiniecki A et al. (1981) Down syndrome fibroblasts are hyperresponsive to beta-adrenergic stimulation. *Proc Natl Acad Sci USA* 78:7670–3
- Mohammadi AA, Bakhshaeekia A, Alibeigi P et al. (2009) Efficacy of propranolol in wound healing for hospitalized burn patients. *J Burn Care Res* 30:1013–7
- Nagatsu T, Levitt M, Udenfriend S (1964) Tyrosine hydroxylase. The initial step in norepinephrine biosynthesis. *J Biol Chem* 239:2910–7
- Pullar CE, Chen J, Isseroff RR (2003) PP2A activation by beta2-adrenergic receptor agonists: novel regulatory mechanism of keratinocyte migration. *J Biol Chem* 278:22555–62
- Pullar CE, Grahn JC, Liu W et al. (2006a) Beta2-adrenergic receptor activation delays wound healing. *FASEB J* 20:76–86
- Pullar CE, Isseroff RR (2005) Cyclic AMP mediates keratinocyte directional migration in an electric field. *J Cell Sci* 118:2023–34
- Pullar CE, Isseroff RR (2006) The beta 2-adrenergic receptor activates promigratory and pro-proliferative pathways in dermal fibroblasts via divergent mechanisms. *J Cell Sci* 119:592–602
- Pullar CE, Rizzo A, Isseroff RR (2006b) Beta-adrenergic receptor antagonists accelerate skin wound healing: evidence for a catecholamine synthesis network in the epidermis. *J Biol Chem* 281:21225–35
- Renshaw SA, Loynes CA, Trushell DM et al. (2006) A transgenic zebrafish model of neutrophilic inflammation. *Blood* 108:3976–8
- Romana-Souza B, Nascimento AP, Monte-Alto-Costa A (2008) Low-dose propranolol improves cutaneous wound healing of burn-injured rats. *Plast Reconstr Surg* 122:1690–9
- Romana-Souza B, Nascimento AP, Monte-Alto-Costa A (2009a) Propranolol improves cutaneous wound healing in streptozotocin-induced diabetic rats. *Eur J Pharmacol* 611:77–84
- Romana-Souza B, Nascimento AP, Monte-Alto-Costa A (2009b) Propranolol improves cutaneous wound healing in streptozotocin-induced diabetic rats. *Eur J Pharmacol* 611:77–84
- Romana-Souza B, Otranto M, Vieira AM et al. (2010a) Rotational stress-induced increase in epinephrine levels delays cutaneous wound healing in mice. *Brain Behav Immun* 24:427–37
- Romana-Souza B, Porto LC, Monte-Alto-Costa A (2010b) Cutaneous wound healing of chronically stressed mice is improved through catecholamines blockade. *Exp Dermatol* 19:821–9
- Romana-Souza B, Santos JS, Monte-Alto-Costa A (2009c) Beta-1 and beta-2, but not alpha-1 and alpha-2, adrenoceptor blockade delays rat cutaneous wound healing. *Wound Repair Regen* 17:230–9
- Rossiter H, Barresi C, Pammer J et al. (2004) Loss of vascular endothelial growth factor activity in murine epidermal keratinocytes delays wound healing and inhibits tumor formation. *Cancer Res* 64:3508–16
- Rough J, Engdahl R, Opperman K et al. (2009) Beta2 adrenoceptor blockade attenuates the hyperinflammatory response induced by traumatic injury. *Surgery* 145:235–42
- Schallreuter KU, Wood JM, Lemke R et al. (1992) Production of catecholamines in the human epidermis. *Biochem Biophys Res Commun* 189:72–8
- Shaw TJ, Martin P (2009) Wound repair at a glance. *J Cell Sci* 122:3209–13
- Sivamani RK, Pullar CE, Manabat-Hidalgo CG et al. (2009) Stress-mediated increases in systemic and local epinephrine impair skin wound healing: potential new indication for beta blockers. *PLoS Med* 6:e12
- Smith EJ, Staton CA (2006) *Angiogenesis Assays*. New York: Wiley
- Souza BR, Santos JS, Costa AM (2006) Blockade of beta1- and beta2-adrenoceptors delays wound contraction and re-epithelialization in rats. *Clin Exp Pharmacol Physiol* 33:421–30
- Steele SL, Yang X, Debiais-Thibaud M et al. (2011) *In vivo* and *in vitro* assessment of cardiac (beta)-adrenergic receptors in larval zebrafish (*Danio rerio*). *J Exp Biol* 214:1445–57
- Steinkraus V, Steinfath M, Korner C et al. (1992) Binding of beta-adrenergic receptors in human skin. *J Invest Dermatol* 98:475–80
- Steinle JJ, Cappocia Jr FC, Jiang Y (2008) Beta-adrenergic receptor regulation of growth factor protein levels in human choroidal endothelial cells. *Growth Factors* 26:325–30
- Tonnesen MG, Feng X, Clark RA (2000) Angiogenesis in wound healing. *J Invest Dermatol Symp Proc* 5:40–6
- Wallukat G (2002) The beta-adrenergic receptors. *Herz* 27:683–90
- Werner S, Grose R (2003) Regulation of wound healing by growth factors and cytokines. *Physiol Rev* 83:835–70
- Westerfield M (1994) *The Zebrafish Book: A Guide to the Laboratory Use of the Zebrafish (Brachydanio rerio)*, 2.1 ed. Eugene, OR: University of Oregon Press
- Yoon CS, Jung HS, Kwon MJ et al. (2009) Sonoporation of the minicircle-VEGF(165) for wound healing of diabetic mice. *Pharm Res* 26:794–801
- Zhang XJ, Meng C, Chinkes DL et al. (2009) Acute propranolol infusion stimulates protein synthesis in rabbit skin wound. *Surgery* 145:558–67



This work is licensed under the Creative Commons Attribution-NonCommercial-No Derivative Works 3.0 Unported License. To view a copy of this license, visit <http://creativecommons.org/licenses/by-nc-nd/3.0/>